Combustion and Flame 191 (2018) 500–512

Contents lists available at ScienceDirect

Combustion and Flame

journal homepage: www.elsevier.com/locate/combustflame

Fire behavior in chaparral–Evaluating flame models with laboratory data

David R. Weise[a,*], Thomas H. Fletcher[b], Wesley Cole[b], Shankar Mahalingam[c], Xiangyang Zhou[d], Lulu Sun[e], Jing Li[f]

[a] USDA Forest Service, PSW Research Station, Fire and Fuels Program, Riverside, CA, USA
[b] Chemical Engineering Department, Brigham Young University, Provo, UT, USA
[c] College of Engineering, The University of Alabama in Huntsville, Huntsville, AL, USA
[d] FM Global, MA, USA
[e] College of Engineering, Embry-Riddle Aeronautical University, Daytona Beach, FL, USA
[f] Department of Fire Science and Professional Studies, University of New Haven, West Haven, CT, USA

A R T I C L E I N F O

Article history:
Received 18 December 2017
Revised 19 January 2018
Accepted 14 February 2018
Available online 7 March 2018

Keywords:
Flame length
Flame angle
Mass loss
Heat release
Chaparral
Wildland fire

A B S T R A C T

Flame and mass loss data for chaparral, a mixture of shrub plants from the Mediterranean climate zone of southwestern North America, from five previously reported experiments were used to evaluate several published models relating flame characteristics to mass loss and heat release rates. These data are unique with fuel moisture content ranging from 0.36 to 0.94 (dry basis); the study used mass loss rates which included water loss. Fit of the data to Froude number correlations developed by Albini, Byram, Nelson and Thomas and heat release rate—flame length correlations by Heskestad, Zukoski, and Yuan/Cox for axisymmetric and line fires were examined.

Chaparral fuels configured as circular cribs and burned in this fashion behaved similarly to other “pool fire” configurations. Scaled flame lengths generally agreed with heat release correlations developed for other fuel types; however, limited agreement for line fire data indicated potential for improvements that can be made. A strong relationship between mass loss rate and flame length in these live fuel beds extends this well-established relationship to these fuel types. The fitted exponent lends support to Byram's derivation that flame length is related to $Fr^{0.5}$ and not Thomas' derivation of $Fr^{2/3}$. Live foliage particles still retain significant moisture at the time of ignition suggesting that moisture content may be an important parameter to include in these correlations if they are to be applied to live wildland fuels.

Published by Elsevier Inc. on behalf of The Combustion Institute.

1. Introduction

The wildland fire flame is the visible manifestation of combustion processes in wildland fuels. This primarily turbulent diffusion flame is a heat source affecting its immediate surroundings. Energy transferred from a flame to the environment can impact plants, animals, soil, water, air and cultural resources in a variety of ways (e.g., [1–7]). Flame size is an important metric that is used in determining fire suppression action and firefighter safety zone size. Fire intensity (which has been correlated to flame length) has been used to predict probability of house survival during bushfires [8]. Flame length is often used as a metric to determine the size of fire control lines [9]. Flame height coupled with distance from the flame has been used to predict the heat flux exposure for wildland fire fighters [10]. Perhaps because of the importance of a fire's flame to man, there is a large body of knowledge related to flame structure and there has been a significant effort in deriving flame models and developing correlative relationships with other fire characteristics [11]. While convective and radiant heat transfer mechanisms in fuel beds have long been recognized and included in physical fire models (e.g., [12]), recent visualization of the details of flow within fuel beds is aiding our understanding of the subtleties and complexities of convection in wildland fuel beds (e.g., [13–15]).

In the United States, G.M. Byram was a pioneer in wildland fire research and contributed in many areas [16]. He developed fire intensity (I) as a measure of heat release and correlated flame length (L) with the simple relation $L = 0.0775I^{0.46}$ [17,18]. The applicability of this correlation has been evaluated in many different wildland fuel types in both laboratory and field settings [19] for spreading fires. Flame data from spreading laboratory fires in the present study were previously compared to Byram's original relation as well as four other statistically-derived correlations for

* Corresponding author.
E-mail address: dweise@fs.fed.us (D.R. Weise).

https://doi.org/10.1016/j.combustflame.2018.02.012
0010-2180/Published by Elsevier Inc. on behalf of The Combustion Institute.

Nomenclature

Roman symbols

c_p	specific heat (kJ kg^{-1} K^{-1})
D	characteristic length: leaf diameter (D_l), pan diameter (D_p), flame depth (D_f),
Fr_{xy}	Froude number based on flame characteristic length x and wind velocity y
g	gravitational acceleration (m s^{-2})
H	flame height (m): H_α - calculated from flame angle; H_ϕ - calculated from flame angle and slope angle
h_c	heat content of fuel, low heat of combustion (kJ kg^{-1})
I	fireline intensity ($h_c m''R$) (kW m^{-1})
L	flame length (m)
l_y	characteristic flame length (L or H)
m_d	oven-dry fuel mass consumed in flaming front (kg)
$\dot{m}_d$	oven-dry mass loss rate (kg s^{-1})
m''_d	oven-dry fuel loading (kg m^{-2})
m'''_d	oven-dry bulk density (kg m^{-3})
m_g	green fuel mass (includes water) (kg)
$\dot{m}_g$	green fuel mass loss rate (kg s^{-1})
m''_g	green fuel loading (kg m^{-2})
m_w	water mass in fuel (kg)
M	moisture content of solid fuel (m_w/m_d)
MAE	mean absolute error
MB	mean bias
N	mass fraction of unburned fuel in gas mixture; stoichiometric air/fuel mass ratio = kN where k is a fuel specific constant [1]
N_c	Byram's convection number: N_c calculated with U, N_{ce} calculated with effective wind speed U_e
$NMAE$	normalized MAE
p	probability associated with value of test statistic
NMB	normalized MB
$\dot{Q}_c$, $\dot{Q}_c^*$	dimensioned (kW) and dimensionless rate of heat release for circular fuel bed, respectively
$\dot{Q}_l$, $\dot{Q}_l^*$	dimensioned (kW m^{-1}) and dimensionless rate of heat release per unit length, respectively
$\vec{R}$	mean resultant length (magnitude) of resultant vector for a sample of a circular variable, $0 \le \vec{R} \le 1$
r	Pearson product moment correlation coefficient, r^2 is the coefficient of determination
$RMSE$	root mean squared error
S	rate of spread of line fire (m s^{-1})
T	absolute temperature (K)
U	horizontal wind velocity (m s^{-1})
U_e	effective wind velocity combining U and ϕ [60] (m s^{-1})
U_x	characteristic wind velocity (U or U_c)
V	vertical velocity in flat flame burner (m s^{-1})
Z	non-dimensional number derived from modified Froude number; denoted N in [76]

Greek symbols

α	angle of flame from vertical [$\cos^{-1}(H/L)$] (degrees)
β	fuel gas mass produced per unit of fuel bed mass loss
γ	linear regression coefficients
δ	fuel bed depth (m)
ζ, η	entrainment coefficients, ζ, denoted α in [58]
θ	$\alpha + \phi$, sum of flame angle and slope angle (degrees)
κ, μ	concentration parameter and mean of von Mises distribution, respectively
λ	nonlinear regression coefficients
ν	kinematic viscosity of air (m^2 s^{-1})
ρ	density (kg m^{-3})
ρ_c	measure of model fit for circular regression
υ	circular standard deviation
ϕ	angle between horizontal and axis of tilted fuel bed (slope) (degrees)
χ^2	$\sum \frac{(\text{observed}-\text{predicted})^2}{\text{predicted}}$, chi-squared statistic

Subscripts

a	ambient conditions

similar shrub fuel types [20]. The chaparral data were found to be most similar to Galician shrublands [21], while the other models underestimated L. Additional work by Byram included the development of scaling laws [22–24] for the fire plume in crossflow by proposing a dimensionless convection number N_c which is a ratio of the power of wind and power of the fire as a measure of the potential for a wildland fire to "blow up" Eq. (1). The quantity N_c was subsequently shown to be proportional to a Froude number based on flame height ($U^2g^{-1}H^{-1}$) [25–29]. Byram used ambient atmospheric properties of density, temperature and specific heat (ρ_a, T_a, c_{pa}) in this derivation.

$$N_c = 2gI/\left[\rho_a c_{pa} T_a (U-S)^3\right] = 2gh_c m'' S/\left[\rho_a c_{pa} T_a (U-S)^3\right] \quad (1)$$

Over 50 years of experiments and modeling have established the correlation of a scaled flame height (H/D) with the Froude number using burner diameter or flame depth (D_f) as the characteristic length (D) for axisymmetric and linear fires, respectively [26,30–33]. Flame data from wildland fuels have been included in this development; however, the wildland fuels have typically been dead fuels such as wood and cast foliage—not living fuels such as shrubs and trees. Nelson [27] cited examples where N_c had been applied to spotting (embers) and crown fire spread—by definition crown fires typically spread through live fuels. Recent work has examined and modeled Froude-based flame geometric relationships in European shrub lands [34–37].

Wildland fuels include living vegetation and the dead foliar and wood components that are either retained on the plant or deposited on the ground. While the emphasis on wildland fuels has been on the dead component, fires burning in living vegetation are a significant portion of the wildland fires, which occur worldwide. In regions of the world where Mediterranean climates occur, wildland fuel often consists of shrubs, which can exhibit significant fire behavior. Shrub fuels are not restricted to Mediterranean regions and include sagebrush in the interior western United States and southern rough in the southeastern U.S. Chaparral is a plant community containing many species of shrubs that grow in the Mediterranean climate region of the U.S. located in California and northern Baja Mexico [38].

As part of a larger program studying fire spread mechanisms in live fuels with an emphasis on chaparral vegetation, experimental work has been conducted at Brigham Young University (BYU), the University of California at Riverside (UCR), and the USDA Forest Service Forest Fire Laboratory (FFL) in Riverside, CA, USA since 2001. Work at BYU developed a flame angle (α)—Froude number correlation for single live and dead leaves in cross-flow for a variety of shrub species [39] and work at UCR examined the relationship between H and heat release rate for pans of live and dead foliage and branches from chaparral species [40]. While fire spread experiments have been conducted at both the fuel bed and field scale in chaparral fuels [41–43], the relationships between flame characteristics and heat release or mass loss have not been explored extensively across this range of scale. This paper compares laboratory data ranging from single leaf to fuel bed scale experiments with several existing relationships developed for wooden cribs and dead foliage. High water content is an important characteristic of live fuels. When the moisture content (M, dry mass basis) of living vegetation exceeds 56%, the majority of a fire plume's water vapor comes from vaporization of water and not the water produced by the combustion reaction [17] so the mass loss rate used in this study is based on the green fuel ($\dot{m}_g$), not dry fuel ($\dot{m}_d$). The experiments that generated the chaparral flame data (Section 2.1) and the models evaluated or developed with the data are described (Sections 2.2, 2.3). Results for flame length—mass loss relationships (Section 3.1); wind velocity effects on flame length, height, and angle (Section 3.2); flame length and heat release rate (Section 3.3); and convection number and Froude number correlations (Section 3.4) follow. A nomenclature is provided.

2. Methods

2.1. Experimental setups

Materials for all chaparral experiments at BYU, UCR, and FFL were collected at the North Mountain Experimental Area located 50 km east of Riverside, CA at an elevation of 1160 m. Data used in this paper are available through the USDA Forest Service Research Data Archive (https://www.fs.usda.gov/rds/archive/). Samples of chaparral were cut and sent by express mail to BYU. Four species were examined: Eastwood's manzanita (*Arctostaphylos glandulosa* Eastw.), scrub oak (*Quercus berberidifolia* Liebm.), hoaryleaf ceanothus (*Ceanothus crassifolius* Torr.) and chamise (*Adenostoma fasciculatum* Hook. & Arn.), representing a wide range of physical characteristics for species comprising chaparral. Flame height (H) and mass loss rate ($\dot{m}$) data in the present paper were estimated during the steady burning period of each set of experiments. The mass loss data recorded in all experiments included green fuel mass (m_g). Our previous work has shown that live fuels such as leaves contain significant amounts of water at the time of ignition [44,45]. In the BYU and UCR experiments, the fuel bed slope ϕ was zero.

The experimental apparatus at BYU was designed to closely resemble the conditions of a forest fire flame front [46]. The fuel sample (a leaf or branch (chamise)) was attached to a stationary horizontal rod connected to a cantilever-type mass balance. A flat-flame burner (FFB) was positioned on a moveable platform to simulate the flame front. The platform was pulled at a constant velocity toward the fuel sample. The post-flame gases from the FFB provided heat transfer by convection. The post-flame gas vertical velocity V was 1 m s^{-1} and the gas temperature was 1273 K. Using leaf diameter (D_l) as the characteristic dimension D resulted in the Reynolds number (VD/ν) for the vertical flow over the leaf ranging from 46 to 721 indicating that the leaves were heated by forced convection that was laminar in character. A video camera and mid-wave infrared (MWIR) camera recorded each experiment. The infrared imagery was used to estimate the surface temperature of the leaf; the flame was not visible in the MWIR. Flame height was determined by averaging measurements of maximum flame height from still images taken from the video.

To examine the effects of horizontal wind velocity (U) on flames from green and dry leaves, the FFB apparatus was modified by adding a fan in a square duct with a honeycomb mesh to provide cross flow of 0.77 to 2.8 m s^{-1} [39]. Assuming these cross-flow velocities only and an average gas temperature of 800 K produced a range of Reynolds numbers of 126 to 795 indicating that the horizontal cross-flow velocities over the leaf were also laminar in character. While the work at BYU included other species common to Utah and the southern U.S. [39,44,47], we used only data from the green manzanita leaves, a chaparral species, in the present study.

Fig. 1. Circular crib fire created by burning solid fuel composed of chamise branches and foliage.

Color imagery of some of the combustion behavior revealed interesting phenomena during the heating, ignition and burning of the green leaves, such as bursting and boiling not typically observed in dead fuels [44,48].

At UCR, cribs of green and dry chaparral fuels were placed in circular pans on an electronic scale and ignited (Fig. 1), [40]. Pan diameters (D_p) of 0.3, 0.45, and 0.6 m and a constant dry fuel loading m''_d of 2.12 kg m^{-2} were used. These fuel beds differed from traditional fuel cribs in that the arrangement of the fuels was not regular (e.g., [49,50]). A constant pan depth of 0.2 m resulted in constant bulk density m'''_d of 10.6 kg m^{-3}. Each pan was ignited using an alcohol-soaked paper towel placed in the bottom of the pan under the chaparral fuel. The amount of alcohol-saturated paper, determined by trial and error, was sufficient to ignite the fuel bed without great perturbation of the fire behavior of the chaparral fuel bed [40].

A height marker placed adjacent to the scale provided a reference scale. A video camera and thermal infrared camera recorded each experiment. Flame height was determined by averaging mea-

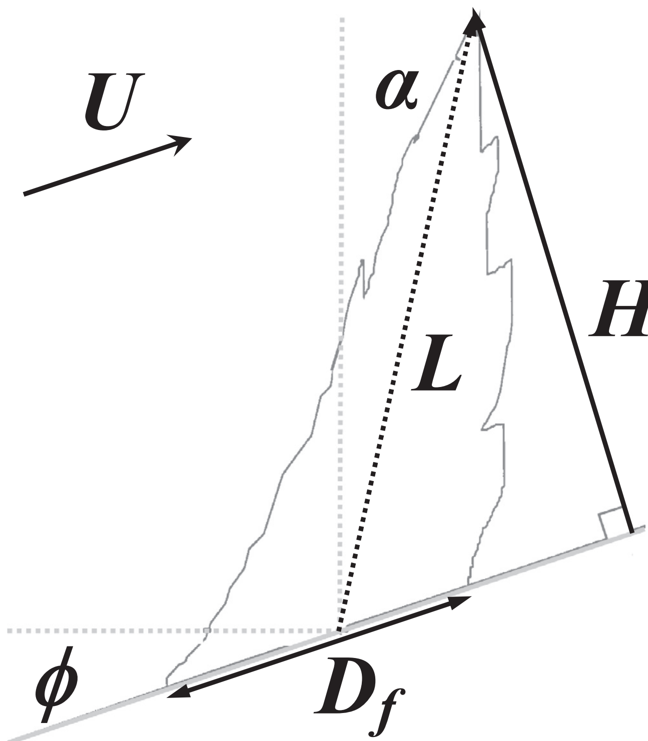

Fig. 2. Components of the diffusion flame resulting from the burning of wildland fuels for a fire spreading on sloped ground.

surements of maximum flame height from still images taken from the video after the alcohol and paper were consumed. For these experiments, characteristic dimension was D_p.

A set of experiments performed in an open-topped wind tunnel at FFL examined the effects of bulk density, wind and ignition location on fire spread in individual shrubs [(dataset) 51,52]. Hosseini et al. [53] provide a detailed description of the fire laboratory and wind tunnel characteristics are available elsewhere [54,55]. Twenty-four individual chamise shrubs were ignited with a line fire or spot fire and with or without a 1.5 m s^{-1} cross-flow. The moisture content M of the live fuel sample was estimated using an Arizona Instruments MAX® 1000 Moisture Analyzer[1]. Shrub mass was measured by an electronic balance. A video camera captured images at a frequency of 30 Hz. Because of fluctuations in the mass data, maximum mass loss rate ($\dot{m}_g$) was calculated by averaging 10 adjacent data points centered about the maximum. L and α were obtained from analysis of at least three video camera images per experiment using AutoCAD. Based on measurements of shrubs harvested to develop bulk density-height models for manzanita and chamise, we calculated the geometric mean of crown diameter measurements yielding $D = 0.6m$ for these experiments. Some aspects of these experiments have been modeled [54,56,57] using LES (large eddy simulation).

The effects of wind (U), moisture content (M), fuel bed depth (δ) and slope angle (ϕ) on flame propagation in live fuel beds were studied at FFL (Fig. 2) using fuel beds (2.0 m long × 1.0 m wide × various depths) constructed of live branch material <0.64 cm and foliage material [41,42, (dataset) 58]. The fuel beds were elevated above the surface of a tilting platform by 0.4 m to simulate an aerial fuel. Air could be entrained from the ends of fuel beds; metal sheeting prevented air entrainment from the sides to reduce the curvature of the flame front and simulate a line fire. Plant material was generally collected in the morning so as to minimize moisture loss through transpiration. Dead fuel was removed to the extent possible. Dry bulk density m_d''' ranged from 6.26 to 14.01 kg m^{-3}; reported natural bulk density of chaparral canopies ranged from 0.4 to 3 kg m^{-3} [59]–values significantly lower. The slope (100tan ϕ) of the fuel beds ranged from −60 to 70% where negative values indicate fire spread downhill [29,42]. A fuel bed was ignited along the 1 m side with an ignition zone of 50 cm depth. Between 0.3 and 0.4 kg of excelsior and a small amount of isopropyl alcohol were added uniformly in the ignition zone to initiate and sustain the ignition. A video camera recorded each experiment and several images during the steady burning phase (near 1 m) were digitized to measure flame characteristics including height, length, depth, and angle. Mass loss rate $\dot{m}_g$ was estimated by combining green fuel loading m_g'', rate of spread S and flame depth (D_f) (Eq. (2)). For the fuel bed data, the characteristic dimension was flame depth D_f. The effects of slope angle ϕ were incorporated by calculating an "effective wind speed" U_e [60].

$$\dot{m}_g = m_g'' S D_f \tag{2}$$

When aggregated, the five data sets contained 576 observations of fire behavior in chaparral fuels. However, some of these studies examined the differences between green and dried foliage [39,40,61] so only data in which $M >= 0.35$ (nominal M for saturated dead woody fuel) were included in the present study. The interested reader is referred to [62] for a good review of the differences in moisture relations between dead and live fuels; [63] provides the theoretical development of drying in dead fuels which formed a basis for fire danger rating in the United States.

2.2. Flame relations

The relationship between mass loss rate and flame length was examined initially. Scatterplots suggested potential statistical relationships which we fit using linear and nonlinear regression. We compared observations with predictions from the empirical models of Byram [22] (Eq. (3)), Fons et al. [64] (Eq. (4)) and Thomas [65] (Eq. (5)) as reported in [[26], Eq. 40–42]. Note that the results for Eq. (3)–(5) were converted to SI units after calculation. The sources of these equations did not specify that mass was oven-dry mass; however, that may have been an unwritten assumption. In order to evaluate the application of Eqs. (3)–(10))\ to flame characteristics from live fuels, we used green fuel mass loss rate ($\dot{m}_g$) for mass loss rate ($\dot{m}$).

$$L = 3.22\dot{m}^{0.46} \tag{3}$$

$$L = 3.13\dot{m}^{2/3} \tag{4}$$

$$L = 3.94\dot{m}^{2/3} \tag{5}$$

For wind-driven fires on flat ground ($\phi = 0$), Albini [26] presented correlations for flame dimensions from Thomas [25] and reported good agreement between observed and predicted of H and α for dead pine needle fuels using modeled thermochemical properties [66]. These correlations are:

$$\begin{aligned} H &= 101\dot{m}U^{-0.74}D^{-0.13} \\ L &= 10.25\dot{m}^{0.86}U^{-0.22}D^{-0.18} \\ \alpha &= \cos^{-1}\left(4.38\dot{m}^{0.14}U^{-0.78}D^{0.18}\right) \end{aligned} \tag{6}$$

Since these correlations resulted from fire spread in wooden cribs with wind we used fuel bed data with $U_a = 2$ m s^{-1} to evaluate these correlations. The BYU individual leaf data (all plant species) [39] have previously been compared to other existing flame angle–Froude number correlations [26,29,67–69]. For

[1] The use of trade or firm names in this paper is for reader information and does not constitute endorsement by the U.S. Department of Agriculture of any product or service.

a given wind velocity, these models derived from single leaf data tended to predict greater flame angles (more deflection from vertical) than the model based on larger-scale data.

We also compared the fuel bed data to Albini's wind-driven flame model [26] given by:

$$H = 122N\beta \dot{m} U_a^{-1}$$
$$\alpha = \tan^{-1}\left(0.0036 U_a H^{-1/2}\right) \tag{7}$$

Since modeling results have shown that the presence of water vapor in the combustion gas mixture reduced maximum temperature of the flame and reactions were quenched when the water mole fraction exceeded 0.65 [70], we incorporated the effect of moisture content M on the fuel gas production ratio β and the stoichiometric air/fuel ratio N using the curves for manzanita and chamise foliage [66] which are available only graphically. Linear regression models for β and N of the form $\beta(\text{or}\, N) = \gamma_0 + \gamma_1 M + \gamma_2 M^2$ were fit to visually-estimated data points measured from the published curves. This model has an additional term when compared to the simple linear equations for white and ponderosa pines [26]. Albini [66] assumed a linear relationship for moisture content M over the range of 0.02 to 0.15 [71,72]. In the case of chaparral fuel beds M ranged from 0.26 to 0.91; Albini's thermochemical curves [66] contain significant curvature over this range. Linear correlation between observed and predicted flame dimensions was estimated using the Pearson product moment correlation coefficient (r) [73].

2.3. Heat release rate

For buoyant diffusion flames from circular burners and square cribs, flame height H has been correlated with the heat release rate ($\dot{Q}_c$) by several authors [11,74]. In the present study, we chose two correlations which have been developed for a wide range of fuels (Eq. (8) [31,75], Eq. (9) [11,76,77]). In these approximate axisymmetric configurations, the characteristic length D is burner diameter. For a line burner (or line fire) with turbulent flames and heat release rate greater than 30 kW m^{-1}, heat release rate ($\dot{Q}_l$) and H have been correlated by Eq. (10) [33]. The pan and shrub data (see Section 2.1) have previously been compared with $\dot{Q}_c^*$ [40,57]. Note that Byram's fireline intensity I [17] which is calculated for a spreading wildland fire has the same units as $\dot{Q}_l$. Further note that Byram developed a correlation $H = 0.0775 I^{0.46} = 0.0775 \dot{Q}_l^{0.46}$ [17] used in operational fire spread models in the United States [78,79]. which is not dimensionless; the exponent is closer to 2/5 than to 2/3. We evaluated the fit of Eqs. (8) and (9) to the leaf, pan and shrub data and the fit of Eq. (10) to the fuel bed data assuming air properties at 25 °C, an effective heat of combustion $h_c = \Delta h_{c,eff} = a - 0.057M$ where $a = 16.77$ and 16.31 kJ g^{-1} for chamise and manzanita, respectively, in place of 16.52 in Babrauskas' original regression fit for Douglas-fir trees [80] and $\dot{Q} = h_c \dot{m}$ [40,66].

$$H/D = Q_c{}^* = \frac{\dot{Q}_c}{\rho_\infty c_p T_\infty \sqrt{gD}\, D^2} = \frac{h_c \dot{m}}{\rho_\infty c_p T_\infty \sqrt{gD}\, D^2} \tag{8}$$

$$H/D = -1.02 + 15.6 Z^{1/5} = -1.02 + 15.6\left[\frac{c_p T_\infty \dot{Q}_c^2}{g\rho_\infty^2 D^5 (h_c/N)^3}\right]^{1/5}$$
$$\approx -1.02 + 3.7 \dot{Q}_c^{*2/5} \tag{9}$$

$$H/D = 3.46 \dot{Q}_l^{*2/3} = 3.46\left(\frac{\dot{Q}_l}{\rho c_p T \sqrt{gD}\, D}\right)^{2/3} = 3.46\left(\frac{I}{\rho c_p T \sqrt{gD}\, D}\right)^{2/3} \tag{10}$$

Prior to carrying out an analysis of the flame angle correlations, the statistical properties of α were examined. Summary statistics were calculated and the fit of the Von Mises distribution ("circular normal") to the data was tested [81]. The exploratory data analysis indicated that the fuel bed and shrub data could be modeled by the Von Mises distribution, but the leaf data could not. As a result the equality of $\bar{\alpha}$ between fuel sizes was tested using a multiple comparison procedure based on the Mardia–Watson–Wheeler uniform score test and adjusting the probability levels to take into account the number of comparisons to control experiment-wise error rate at 0.05 [82]. This test was also used to test equality of flame angle predictions and observed data.

All correlations presented above assume a horizontal orientation of the fuel bed or $\phi = 0$. While extensive work has examined fire spread on vertical surfaces, this seldom, if ever occurs in wildland fires. Recent work by Nelson [83] applied to the results reported by [34] presented Froude numbers modified to take into account the combined effects of U and ϕ using an effective wind speed $U_e = U + (2gI/\rho_a c_{pa} T_a)^{1/3} \sin(\phi)$ [60]. Figure 2 reflects this geometry. The relationships between various Froude numbers based on L, H_α and H_ϕ coupled with U and U_e and flame angle were examined using the fuel bed data and the general form of the Froude number $Fr_{xy} = (U_x - S)^2/gl_y$. For $U_x - S < 0$, $Fr_{xy} = 0$ and $N_c = \infty$. Typically the Froude number has been related to the tangent of the flame angle using a simple linear regression of the formtan$(\theta) = \gamma_0 + \gamma_1 Fr_{xy}$ where $\theta = \alpha + \phi$. Analysis of circular data has advanced to the point that a circular variable can be regressed on linear variables through a link function involving tan^{-1} so we fit the linear-circular model $\theta = \gamma_0 + \gamma_1 Fr_{xy}$ using circular-linear regression [81,84].

Goodness of fit of the regression models was assessed using a variety of measures. Mean absolute error (MAE), normalized MAE (NMAE), mean bias (MB), normalized MB (NMB) and root mean squared error (RMSE) provide measures of agreement [20,85]. The commonly-used coefficient of determination (r^2) is not appropriate to use with nonlinear regression or regression through the origin models [86,87]. To describe the variation accounted for by the fitted models which were not traditional linear regressions, an alternative r^2 was calculated: $r^2_{LR} = \sum \hat{Y}_i^2 / \sum Y_i^2 = 1 - (SSE/SST)$ where SSE and SST are the residual and total sum of squares, respectively. Statistical analyses and graphing were performed using R version 3.4.1 [88].

3. Results and discussion

Combining the five data sets resulted in a total of 496 observations for chaparral fuels (Table 1). Moisture content M ranged from 0.36 to 0.94; the minimum is lower than the minimum observed in the Los Angeles County live fuel moisture data (0.56) [89]. We attribute this difference to moisture loss in transport and sampling variability [90]. The range of observed wildland fire behavior in chaparral occurs over the range of M in the present study [91]. Mass loss $\dot{m}_g$ ranged from 0.001 to 68 g s^{-1} and flame length L ranged 0.015 to 4.82 m. The line fires spread at rates up to 0.03 m s^{-1} which is in the lower range of reported S for chaparral wildfires [92,93]. Heat release rate ($\dot{Q}$) ranged from 2 to 1555 kW m^{-2} for the axisymmetric flames and fire line intensity up to 1768 kW m^{-1} for the line fires. The flames in the leaf tests were primarily laminar while the pan, shrub and bed tests produced turbulent flames. Comparison of this data set with data for other fuel types [19] indicated that the range of data for the pan, shrub, and fuel bed fires were comparable to other laboratory and field studies. Unlike the present study, the fuels in the comparison studies consisted of a mixture of live and dead fuels.

Table 1
Summary of some characteristics of chaparral fuel experiments. Values are the minimum and maximum observed.

Source	Size	n[a]	U (m s^{-1})		$\dot{m}_g$ (g s^{-1})		L (m)		α (°)		$\dot{Q}$[b]	
Pickett	Leaf	123	0		0.006	0.063	0.015	0.085	0		2	36
Cole	Leaf	250	0.8	2.8	0.006	0.063	0.025	0.102	32	78	4	39
Sun	Pan	48	0		3.4	52.2	0.47	2.22	0		145	972
Li	Shrub	24	0	1.5	9.1	68.0	0.69	4.82	−16	40	211	1555
Zhou	Fuel bed	51	0	2	0.7	50.6	0.55	2.80	−12	36	54	1768

Note: Head fire data only.
[a] Number of experiments.
[b] For Pickett, Cole, Sun, and Li, units are kW m^{-2}; for Zhou and comparison studies, units are kW m^{-1}.

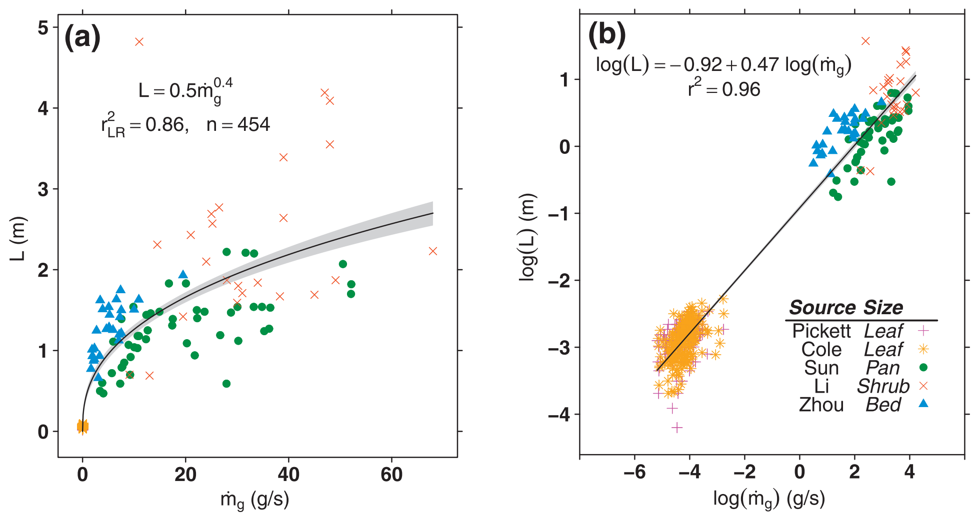

Fig. 3. Relationship between flame length (L) and mass loss rate ($\dot{m}_g$) fitted as a power function using nonlinear least squares (a) and as a log–log model using ordinary least squares (b). The grey band illustrates the 95% confidence interval about each fitted regression.

3.1. Flame length (L) and mass loss rate ($\dot{m}_g$)

A plot (Fig. 3a) of L versus $\dot{m}_g$ suggested a significant relationship for the $\phi = 0$ subset of the data. Using nonlinear regression to fit the general model $L = \lambda_0 \dot{m}_g^{\lambda_1}$, we fit the equation $L = 0.5\dot{m}_g^{0.4}$. The intercept and exponent terms were statistically different from 0 ($p < 0.00001$), the 95% confidence intervals for λ_0 and λ_1 were (0.45, 0.56) and (0.37, 0.43), respectively. The nonlinear regression accounted for 86% of the total variation (r^2_{LR}) in L. We previously reported significant regressions of L as a function of $\dot{Q}^{0.4}$ which implied $\dot{m}^{0.4}$ since we assumed a constant h_c for the pan data [40]. For leaf data for a wide variety of species, flame height was a power function of mass loss; however, the model did not account for much of the variability [61]. For the fuel bed data, we previously fit a similar nonlinear equation ($L = 0.2I^{0.34}$) relating flame length to fireline intensity based on m_d'' [20]. In the present study a log–log plot revealed a significant linear relationship (Fig. 3b) accounting for 96% of the variation in L after correcting for mean L (r^2). The goodness of fit measures (error metrics) for the nonlinear regression and the linear regression of the log–log transformed data were similar (Table 2). The goodness of fit measures for the log–log linear regression were calculated by transforming the predicted log (L) back to L in order to be comparable with the measures for the nonlinear model. Normalizing the flame length data using the appropriate D did not reduce the scatter of the data.

Of the three empirical flame equations, Byram's (Eq. (3)) fit the data best with the smallest error metrics (Table 2). Thomas and Fons tended to over predict the data due to the greater exponent (2/3) which Albini [26] reported for his data (Fig. 4). The fuel moisture M for the wooden cribs ranged from 0.04 to 0.16—a typical range for dead fuels that burn [64,65]. As noted earlier in

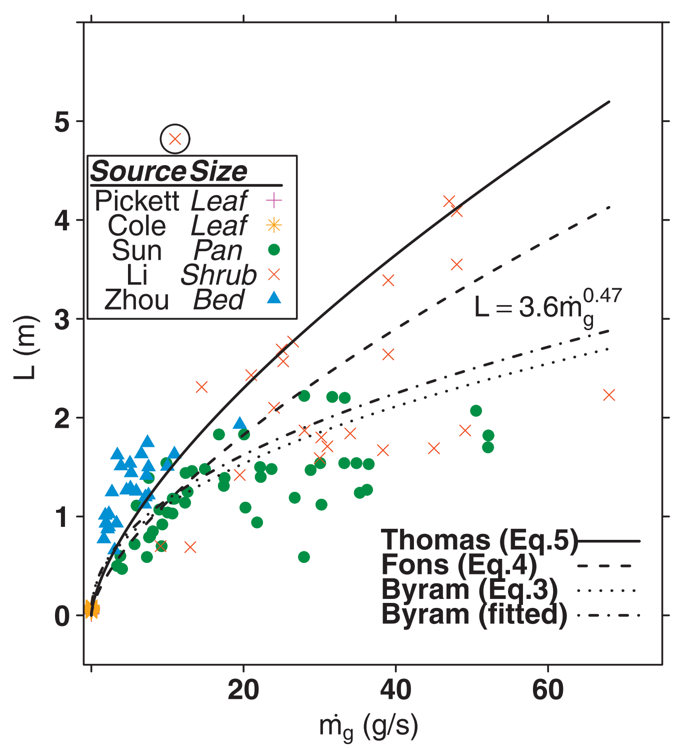

Fig. 4. Comparison of existing flame length-mass loss correlations (Eq. (3)–(5)) using laboratory-scale fires in chaparral fuels.

Table 2
Summary of goodness of fit of various equations for laboratory-scale fire behavior data from burning chaparral foliage. Mean absolute error (MAE), normalized MAE (NMAE), mean bias (MB) and root mean squared error (RMSE) defined in [20]. Normalized MB (NMB) is $MB/\bar{y}$ where y is the measured flame length L. MAE, MB, and RMSE have units, NMAE and NMB are proportions.

Correlation			MAE	NMAE	MB	NMB	RMSE
$L = 0.5\dot{m}_g^{0.4}$		(m)	0.13	0.35	0.02	0.06	0.30
$\log(L) = -0.92 + 0.47\log(\dot{m}_g)$		(m)	0.11	0.30	−0.02	−0.05	0.31
Byram (Eq. (3))	$\dot{m}_g$	(m)	0.50	1.32	0.49	1.30	1.06
	$\dot{m}_d$	(m)	0.33	0.86	0.31	0.84	0.72
Fons (Eq. (4))	$\dot{m}_g$	(m)	1.04	2.77	1.04	2.75	2.66
	$\dot{m}_d$	(m)	0.68	1.80	0.65	1.72	1.76
Thomas (Eq. (5))	$\dot{m}_g$	(m)	1.40	3.72	1.40	3.72	3.52
	$\dot{m}_d$	(m)	0.93	2.46	0.91	2.42	2.39
Fitted Byram	$\dot{m}_g$	(m)	0.11	0.30	−0.02	−0.05	0.31
Thomas (Eq. (6))	L	(m)	0.34	0.40	−0.30	−0.36	0.95
	H	(m)	0.37	0.54	−0.37	−0.54	1.08
	α	(°)	37	0.71	37	0.71	39
Albini (Eq. (7))	H	(m)	0.16	0.73	−0.16	−0.73	0.44
	α	(°)	34	0.66	34	0.66	36

Table 3
Summary of fitted regression models to estimate fuel gas mass (β) and the stoichiometric air/fuel mass ratio for fuel gas (N) using Albini's thermochemical model [1]. The general regression model was Property $= \gamma_0 + \gamma_1 M + \gamma_2 M^2$ where M is moisture content.

Property	Species	γ_0	γ_1	γ_2	r^2
β	Chamise	1.873	0.0207	−1.0E-4	0.925
	Manzanita	1.938	0.0168	−6.7E-5	0.876
N	Chamise	2.357	−0.0484	2.9E-4	0.944
	Manzanita	2.235	−0.0462	2.8E-4	0.940

Table 4
Summary statistics of observed and predicted flame angles (α, °) for chaparral fuels. $\hat{\upsilon} = [2(1-\bar{R})]^{1/2}$ where $\bar{R}$ is the mean resultant length [84].

Statistics	Leaf	Shrub	Fuel bed
Sample size	233	12	12
Observed mean $\bar{\alpha}$	55	29	22
Standard deviation $\hat{\upsilon}$	0.19	0.10	0.09
Concentration parameter $\hat{\kappa}$	27.6	85.8	144.4
Thomas (Eq. (6)) $\bar{\alpha}$	89	86	88
Thomas $\hat{\upsilon}$	0.005	0.004	0.004
Albini (Eq. (7)) $\bar{\alpha}$	88	31	68
Albini $\hat{\upsilon}$	0.02	0.10	0.10

this section, M for the chaparral fuels ranged from 0.36 to 0.94 – the upper value is within the upper value for the annual moisture cycle in these live chaparral fuels. Using $\dot{m}_d$ instead of $\dot{m}_g$ reduced the errors but did not change the relative order of the correlations (Table 2). Note the close agreement between the Eq. (3) exponent from [17] and the exponent of the transformed log–log fitted equation (0.46 versus 0.47). Changing units and transforming the fitted log–log equation (Fig. 3b) resulted in $L = 3.6\dot{m}_g^{0.47}$ (Fig. 4). The 95% confidence interval for the exponent 0.47 was (0.46, 0.48).

Note the circled point above the legend. This point was examined as a potential outlier; this data point had the greatest L with a low value of $\dot{m}_g$ but no obvious reason for excluding the point was noted. The shrub was selected in the field randomly and its attributes other than mass were comparable to other shrubs which were harvested from the same area. Given the inherent variation observed in structure and condition in chamise shrubs at the sample location [94], we chose not to eliminate the data point.

3.2. Wind velocity (U) and flame measures (L, H, α)

A total of 257 data points were available to evaluate the relationship between U and flame properties for chaparral fuels with $\phi = 0$. While the regressions to estimate the properties β and N for Albini's flame model [26] for chamise and greenleaf manzanita (*Arctostaphylos patula* Greene) (Table 3) did not account for all of the variability in the visually-extracted data, they captured most of it. These equations can potentially be used in other applications such as [55] where it may be desirable to predict thermochemical properties of live fuels.

Flame height H was consistently underestimated by both Eqs. (6) and (7) (Fig. 5a, b) as indicated by negative MB (Table 2). Analysis of variance and Tukey's HSD multiple comparison test [73] indicated that NMB differed between the fuel sizes; the leaf data had the greatest NMB (−0.94, −0.99) and the shrub data had the smallest NMB for both Eqs. (6) and (7) (−0.34, −0.58). Albini estimates of H (Eq. (7)) for the leaf data were an order of magnitude smaller than Thomas' estimates. Similarly, the NMB for Thomas' flame length L differed between fuel sizes. NMB of the shrub data was much closer to 0 than the other two fuels (−0.11 or 11% underestimation versus −0.43 and −0.87 for shrub, bed, and single leaf fuels, respectively). The dotted line corresponds to observed values equaling predicted values (Fig. 5) and the solid line illustrates the fitted relationship between observed and predicted values. Although the predictions for H and L were biased, significant linear relationships between observed and predicted values were evident suggesting a method to correct the bias.

Observed mean and standard deviation of α varied between fuel types (Table 4). The multiple comparison test indicated that $\bar{\alpha}$ differed significantly between the shrub and fuel bed sizes ($p < 0.03$) and between the leaf and other two fuel sizes ($p < 0.0001$). In contrast, Thomas' correlation (Eq. (6)) consistently predicted large α for the chaparral fuels and was insensitive to fuel size. Its standard deviation was an order of magnitude smaller than both the observed data and Albini's correlation (Eq. (7)). The over prediction and insensitivity of Thomas' correlation for α was consistent with results reported previously by Albini [26]. The Mardia–Watson–Wheeler test indicated that Albini's predictions of flame angle differed significantly between fuel sizes ($p < 0.0001$). Comparison of observed α with Eq. (7) predictions revealed significant differences for the leaf and fuel bed data ($p < 0.0001$), but not for the shrub data ($p > 0.9$). Mean difference was 33° and 46° for the leaf and fuel bed data, respectively, but only 2° for the shrub data (Table 4). The normalized bias and absolute errors for the leaf and fuel bed data were 0.61 and 2.10 (61 and 210%), respectively (Table 5). Normalized values for the shrub data were much smaller. When fuel size was not considered, the bias and

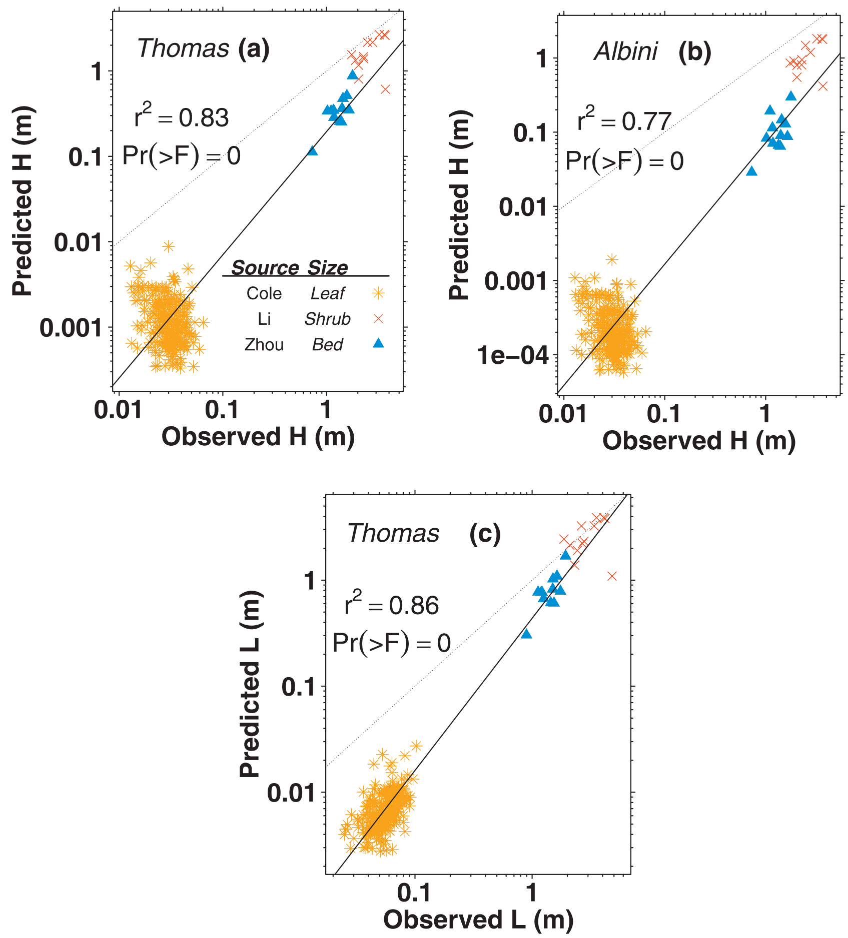

Fig. 5. Comparison of observed and predicted flame sizes for chaparral single leaf, shrubs and fuel beds in cross flow using Albini's approximations of Thomas' correlations (Eq. (6)) for H (a) and L (c) and Albini's flame model (Eq. (7)) for H (b).

Table 5
Summary of goodness of fit of two wind–flame angle (°) correlations by fuel size. Measures defined in Table 2.

Fuel size	Correlation	MAE	NMAE	MB	NMB	RMSE
Leaf	Thomas (Eq. (6))	34	0.62	34	0.62	36
	Albini (Eq. (7))	34	0.61	34	0.61	35
Shrub	Thomas	57	1.94	57	1.94	57
	Albini	17	0.16	17	0.05	18
Bed	Thomas	66	3.01	66	3.01	66
	Albini	55	2.10	55	2.10	56

error of Eq. (7) was 33° resulting in normalized bias and error of 62% (over prediction) (Table 2).

Overall, both Thomas' and Albini's predictive equations of flame angle as a function of wind velocity had similar bias, absolute and root mean squared errors (Table 2). However, when separated by fuel size, the performance differed (Table 5). For the leaf data, performance was similar. For the shrub data, performance of Albini's correlation was superior to Thomas with much smaller bias, absolute error and root mean squared error. In the fuel beds, bias and error of Albini's correlation increased but was still smaller than Thomas' correlation. The use of β and N for green chaparral fuels resulted in α closer to the observed values than Thomas's equation did.

3.3. Heat release rate (Q_c^*, Q_l^*, I) and scaled flame dimension (L/D, H/D)

The relationship between Q_c^* and L/D for the circular configurations appeared to differ by size. The pan data matched the correlation derived by Heskestad [77] well; however, this correlation under-estimated the shrub data and over-estimated the leaf data (Fig. 6a). Padhi's correlation for a statistically stationary modeled fire developed from the shrub data–$4.5\dot{Q}_c^{*0.45}$ [51,52,57] fit these data better and we successfully fit the model $L/D = \lambda_0 Q_c^{*\lambda_1} = 1.93Q_c^{*0.37} \cong 1.9Q_c^{*2/5}$ to the leaf data. The 95% confidence intervals for the λs were (1.80, 2.06) and (0.33, 0.41). The exponent on Padhi's correlation is close to 2/5 but a confidence interval for the exponent estimate was not reported [57]. While the coefficients (λ_0) differed between the present study and earlier studies [40,57] using live chaparral data, there appeared to be support for $\dot{Q}^{*2/5}$. Zukoski [74] identified two regimes: for $\dot{Q}_c^* > 1$ the 2/5 slope (exponent) suggested that L is not affected by D, for $\dot{Q}_c^* < 1$ L is dependent on D and an empirical fit of $\dot{Q}_c^{*2/3}$was developed. For our data, 11 leaf, 11 pan, and 6 shrub fires had $\dot{Q}_c^* < 1$ and 352 leaf, 37 pan, and 18 shrub fires had $\dot{Q}_c^* > 1$. The fitting of a simple linear model to the pan and shrub data did not produce a significant regression ($p > 0.10$) so a segmented regression was performed which estimated the breakpoint where slope would change [95]. For these data, the slope changed appreciably at $\dot{Q}_c^* = 0.49$ where (0.36, 0.61) was the 95% confidence interval of the estimate (Fig. 6b). The previously identified (Section 3.1) circled shrub data

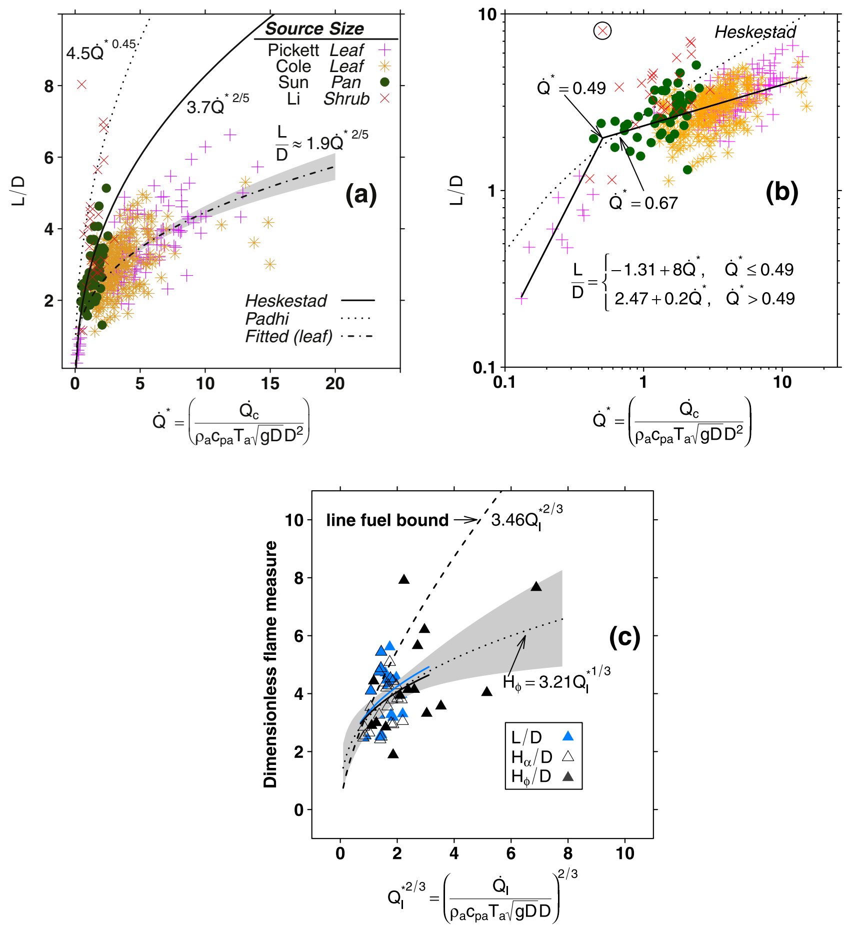

Fig. 6. Relationship between scaled flame length and dimensionless heat release rate for circular fires in axisymmetric fuel beds (a, b) and for line fires in rectangular fuel beds (c). For axisymmetric fuel beds plotted correlations include Heskestad [77], Padhi et al. [57], and a fitted nonlinear regression model (a) and a fitted segmented regression model (b) [95]. For line fires (c), plotted correlations include the "line fuel bound" and fitted nonlinear regression models.

Table 6
Summary of goodness of fit of non-dimensional flame length (m) – heat release rate correlations by fuel size. Measures defined in Table 2.

Fuel size	Correlation	MAE	NMAE	MB	NMB	RMSE
Leaf	Heskestad (Eq. (9))	2.1	0.69	2.1	0.69	2.35
	Padhi [57]	5.0	1.63	5.0	1.63	6.37
	$1.9\dot{Q}_c^{*2/5}$	0.7	0.24	0.2	0.05	0.96
Pan (3)	Heskestad	0.7	0.24	0.4	0.13	0.81
	Padhi	2.4	0.85	2.4	0.85	2.55
	$1.9\dot{Q}_c^{*2/5}$	0.8	0.27	−0.7	−0.23	0.95
Shrub (4)	Heskestad	1.3	0.34	−0.8	−0.20	0.81
	Padhi	1.7	0.44	1.2	0.31	2.14
	$1.9\dot{Q}_c^{*2/5}$	1.8	0.47	−1.8	−0.45	2.42
All	Heskestad	1.4	0.41	0.5	0.17	1.78
	Padhi	3.0	0.92	2.9	0.87	3.56
	$1.9\dot{Q}_c^{*2/5}$	1.1	0.34	−0.8	−0.23	1.61

point was statistically influential; removal of this data point resulted in $\dot{Q}_c^* = 0.67, (0.50, 0.85)$.

Goodness of fit measures of the Heskestad, Padhi and fitted correlations indicated that the fitted correlation ($1.9\dot{Q}^{*2/5}$) was best for the leaf data, an unsurprising result (Table 6). For the pan and shrub data, the Heskestad correlation produced the smallest errors even though the Padhi correlation was developed from the shrub data. To provide equal weighting between fuel sizes (Table 1) to calculate the overall goodness of fit measures, 1000 random samples of 24 observations were drawn from the data for each size class, the measures were summed individually and the mean of each measure was calculated. The fitted leaf correlation had the smallest error measures overall, followed by Heskestad (Eq. (9)) and Padhi's correlation. On a log–log plot, Heskestad fell between the leaf and pan/shrub data (Fig. 6b). For $\dot{Q}_c^* < 1$, the empirically fit exponent for $\dot{Q}_c^*$ was 1 which differs from Zukoski's empirical 2/3.

There was little to no evidence of a linear relationship between $\dot{Q}_l$ and L or H_α (Fig. 6c) for the fuel beds that spread on level ground ($\phi = 0$) as indicated by non-significant F-statistics. For these data $H_\alpha = L\cos(\alpha)$. Nonlinear regression estimated models of the form $\lambda_0 Q_l^{*\lambda_1}$ for L, H_α, and H_ϕ where $H_\phi = L\cos(\alpha + \phi)$ to incor-

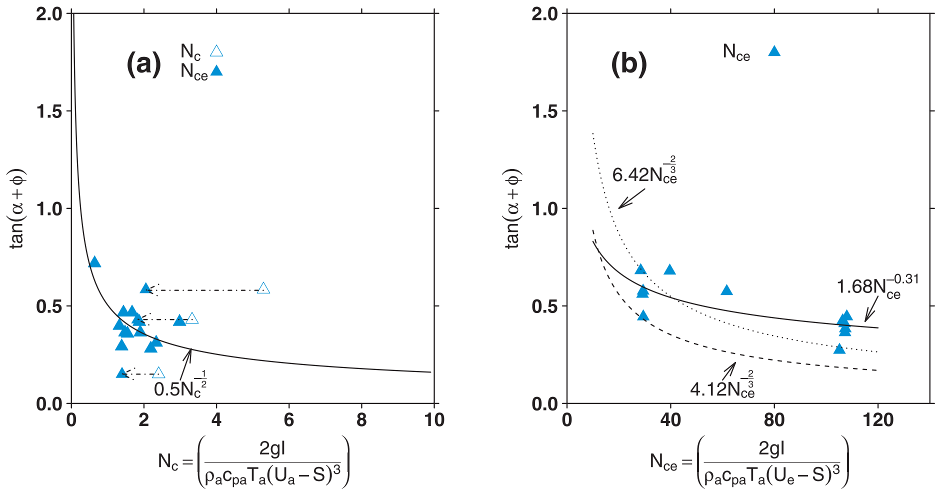

Fig. 7. Relationship between flame angle and Byram's convection number calculated using ambient wind (U_a) and effective wind (U_e) velocity for $N_c < 10$ (a) and $N_{ce} > 10$ (b). N_c was calculated using wind velocity U_a and N_{ce} was calculated using effective wind velocity U_e. Note the difference in range of N_c and N_{ce}.

porate slope angle [60]. The coefficient estimates were similar for L, H_α, and H_ϕ, the t-tests of the estimates were most significant for H_ϕ, and the 95% confidence interval for the H_ϕ regression included the curves for L and H_α. While nearly all of the data fell on or below the "line fuel bound"($3.46Q_l^{*2/3}$), the fitted exponent (1/3) was significantly different for the fuel bed data. The 95% confidence intervals for the λs were (2.54, 3.65) and (0.15, 0.50), respectively. $\dot{Q}_l$ (and I) ranged from 68 to 2297 kW m^{-1} [20] which is well above the minimum heat release rate for the "line fuel" correlation [33]. While the pan data supported the basis for the flame sub-model used by Balbi et al. [96,97], future development of this model should consider using the "line fuel bound" model since it provided an upper bound to the fuel bed data. The geometry of the flame is also more consistent with the assumptions made [96].

3.4. Byram's convection number (N_c) and Froude numbers with flame angle $\alpha + \phi$

Forty-one fires from the Zhou data set with $\phi \geq 0°$, $U_a \geq 0$ were available for these analyses. The convection number N_c (open triangles in Fig. 7a) calculated with U_a was finite for fifteen of the forty-one fires and ranged from 0.6 to 5.3 which meant these fires fell into the intermediate region defined in [83] where heating prior to ignition was a mixture of convection and radiation heat transfer. For the remaining 26 fires, $N_c = \infty$. Use of the effective wind speed U_e [60] significantly increased the range of N_{ce} ($0.6 \leq N_{ce} \leq 108$) and the number of fires with finite N_{ce} to 27. For fires with no wind and a positive slope ϕ, $U_e > 0$ and N_{ce} ranged from 28 to 108 due to the effect of slope alone. Following [98] we used $N_c = 10$ as the breakpoint and regressed $\tan(\alpha + \phi)$ on various powers of N_c and N_{ce}. For the fires with $N_c < 10$, we examined $N_c^{-1/2}$ and $N_{ce}^{-1/2}$ with no intercept term. The slope estimates for $N_c^{-1/2}$ and $N_{ce}^{-1/2}$ of angle 0.52 and 0.50 did not differ statistically based on 95% confidence intervals; however, the residual error of the N_{ce} data was smaller due to the shift of data points resulting from the use of U_e (Fig. 7a). Assuming a slope estimate of 0.5 for the chaparral data yielded an entrainment constant $\eta = 0.13$ which differed from $\eta = 0.71$ for fuel beds of pine litter and palmetto fronds [98, eq. (23)]. One important difference between the pine litter/palmetto fuel beds and the chaparral fuel beds is that the pine needle-palmetto fuel beds were contiguous with the ground which restricted air flow from underneath the burning vegetation. The chaparral fuel beds were elevated; lateral entrainment was blocked, but air flow under the fuel bed was possible. Model simulations demonstrated this flow was significant for fires spreading up slopes [42] which would potentially alter the entrainment constants for these fires.

For $N_c > 10$, Nelson et al. [98] suggested $N_{ce}^{-2/3}$. Reexamination of the fits of the two regressions in their Fig. 2a and b indicated that the 95% confidence intervals for the slope estimates (3.931 and 4.119) overlapped and thus did not differ statistically. The fitted regression (Fig. 7b) for the chaparral data (slope = 6.42) better described the data than the regressions in Nelson et al. [98]. We used nonlinear regression to estimate both the slope and the exponent from the chaparral data; both powers (−1/2, −1/3) derived by Nelson et al. for $N_c < 10$ fell within the confidence interval [−0.51, −0.11] of the exponent estimate (−0.31). Recall that these chaparral N_{ce} values were based solely on slope.

Six Froude numbers were calculated based on L, H_α, and H_ϕ with U_a and U_e: Fr_{LU}, Fr_{LU_e}, $Fr_{H_\alpha U}$, $Fr_{H_\alpha U_e}$, $Fr_{H_\phi U}$, and $Fr_{H_\phi U_e}$. The Froude numbers all occurred in the range $0 \leq Fr_{xy} \leq 0.6$; Froude numbers reported for fires in shrub fuels in France fell in the range $0.13 \leq Fr \leq 0.45$ [37]. For the no wind fires, the Froude numbers based on U were all 0 and there was no linear relationship between flame angle and Froude number (Fig. 8). Froude numbers based on U_e had non-zero values resulting in a linear trend between flame angle and the Froude number. For the circular-linear regressions of the fires with wind, the slope coefficients were highly significant for all Froude numbers with probability values <4E-7 (Table 7). Use of the effective wind speed improved the fit of all regressions as indicated by smaller MAE, NMAE and RMSE measures. On average, the NMAE was reduced by 0.043 (4.3%). The error metrics for Froude numbers based on L were slightly larger than the error measures for H-based Froude numbers; however, when normalized by the mean flame angle, we observed little difference in the predictive capability for flame angle between the Froude numbers based on L versus H.

For the leaf and pan data, there is strong support for the well-established Froude scaling for these live fuels using the mass loss rate that includes water. It may be possible to reduce the scatter in the data by identifying the relationship or characteristic length that will improve the correlation. Fuel moisture, fuel particle shape and thermochemical characteristics are potential variables. The fuel bed data includes non-zero slope and wind effects which may contribute to the scatter. Nelson's recent formulation of Froude num-

Table 7
Summary of circular-linear regressions of flame angle with various Froude numbers for chaparral fuel beds burned with wind. Mean absolute error (MAE) and root mean squared error (RMSE) expressed in radians, normalized MAE (NMAE) is a proportion.

Fr_{xy}	Effective wind velocity	Intercept (γ_0)	γ_1	MAE	NMAE	RMSE
Fr_{LU}		0.138	0.431	0.071	0.188	0.087
Fr_{LU_e}	Y	0.024	0.589	0.054	0.144	0.070
$Fr_{H_\alpha U}$		0.154	0.371	0.065	0.174	0.082
$Fr_{H_\alpha U_e}$	Y	0.049	0.507	0.049	0.130	0.062
$Fr_{H_\phi U}$		0.134	0.402	0.064	0.169	0.079
$Fr_{H_\phi U_e}$	Y	0.062	0.481	0.047	0.126	0.061

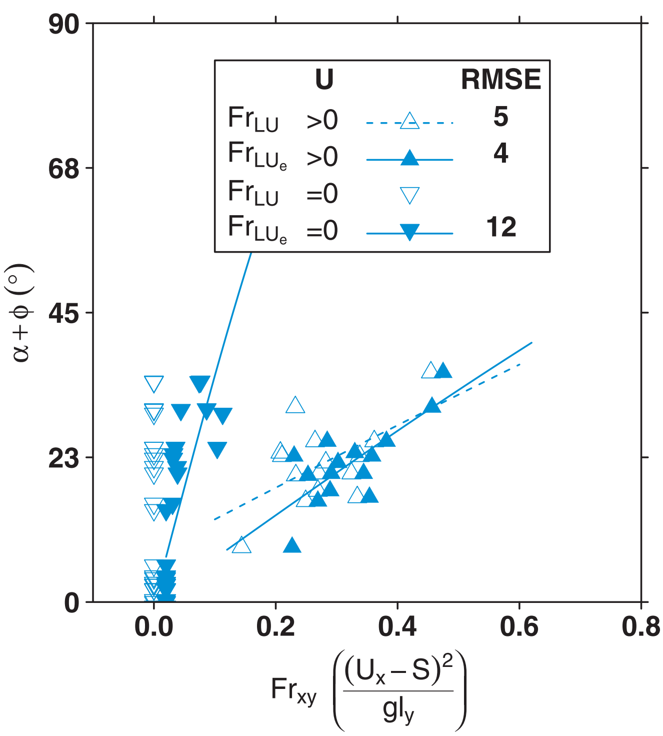

Fig. 8. Circular-linear regressions of flame angle α corrected for slope ϕ and Froude numbers based on flame length L for chaparral fuel beds burned with and without wind velocity. The x-coordinate of the Froude numbers based on U_e has been dithered. The RMSE values in the figure are expressed in degrees.

bers for fires spreading under wind and slope effects [83] improved the correlation with flame angle; Froude numbers based on flame height generally performed better. This limited test coupled with previous results on the effectiveness of U_e in dead fuels [60] suggests that a Froude number based on U_e might be a useful scaling parameter for experiments examining wind and slope effects on fire behavior. If the pan data and the fuel bed data are viewed as cribs, scaling laws developed for wooden cribs based on the fuel particle length might be used to scale the laboratory results to field scale [99]. Factors such as fuel moisture and varying fuel particle shape are perhaps characteristics unique to wildland fire. Most correlations appear to have been developed from fuels where free water in the fuel is not an important component.

4. Conclusion

Chaparral fuels configured as circular fuel beds and burned in this fashion behaved similarly to other "pool fire" configurations. Scaled flame lengths generally agreed with heat release correlations developed for other fuel types. Due to complex topography, changing fuel types, and the vagaries of local meteorology, a wildland fire is seldom a stationary circular fire or an idealized line fire except in small segments. The flame model for a line fire developed by Albini in the late 1970s and early 1980s has seen little validation and development since its introduction. To our knowledge, this is the first time that the parameters developed for chaparral fuels have been tested with limited success. The limited agreement of the heat release rate correlation for a line fire by Yuan and Cox [33] with the chaparral fuel bed data indicates that there are still improvements that can be made. The chaparral fuel bed data were originally collected as part of a study examining marginal fire spread. Only about half of the fires which were ignited spread the entire length of the fuel bed. Several factors were found to be related to fire spread success in these fuel beds; wind velocity was the most important [20]. These marginal conditions and the fact that the fuel beds were elevated resulting in additional entrainment may have contributed to the poor agreement with the data.

The strong relationship between mass loss rate and flame length in these live fuel beds extends this well-established relationship to these fuel types. The fitted exponent lends support to Byram's derivation that flame length is related to $Fr^{0.5}$ and not Thomas' derivation of $Fr^{2/3}$. Live foliage particles still retain significant moisture at the time of ignition [44,45] indicating that the treatment of moisture and its transport in live fuel particles needs to be changed. The amount of water present in fuels may be an important parameter that should be included in these correlations if they are to be applied to live wildland fuels.

Acknowledgments

The measurements reported in this paper resulted from agreements between the USDA Forest Service, Pacific Southwest Research Station, Riverside, CA with Brigham Young University and the University of California-Riverside. The agreements were funded by the USDA/USDI National Fire Plan project 01.PSW.A.3 "Fire behavior in live fuels". The assistance of Dr. Arthur Pewsey, University of Extremadura with the circular-linear regression analysis and the comments of Dr. Ralph Nelson, Forest Service research (retired) regarding flame length and flame height are much appreciated.

References

[1] J.G. Goldammer, V.V. Furyaev (Eds.), Fire in Ecosystems of Boreal Eurasia, Kluwer Academic Publishers, Dordrecht; Boston, 1996.
[2] L.F. DeBano, D.G. Neary, P.F. Ffolliott, Fire's Effects on Ecosystems, John Wiley, New York, 1998.
[3] A. Bytnerowicz, M.A. Arbaugh, C.K. Andersen, A.R. Riebau (Eds.), Wildland Fires and Air Pollution, Elsevier, Amsterdam; Boston, 2009.
[4] A. Cerdà, P.R. Robichaud (Eds.), Fire Effects on Soils and Restoration Strategies, Science Publishers, Enfield, NH, 2009.
[5] M.A. Cochrane, Tropical fire ecology: climate change, land use, and ecosystem dynamics, Springer, Berlin ; New York : Chichester, UK, 2009 Published in association with Praxis Pub.
[6] R.A. Bradstock, R.J. Williams, A.M. Gill, Flammable Australia: fire regimes, biodiversity and ecosystems in a changing world, CSIRO Publishing, Collingwood, Vic., 2012.
[7] J.E. Keeley, W.J. Bond, R.A. Bradstock, J.G. Pausas, P.W. Rundel, Fire in Mediterranean ecosystems: ecology, evolution and management, Cambridge University Press, Cambridge, UK; New York, 2012.
[8] A.A.G. Wilson, I.S. Ferguson, Predicting the probability of house survival during bushfires, J. Environ. Manag. 23 (1986) 259–270.

[9] R. Mees, D. Strauss, R. Chase, Modeling wildland fire containment with uncertain flame length and fireline width, Int. J. Wildland Fire 3 (1993) 179–185.
[10] B.W. Butler, Wildland firefighter safety zones: a review of past science and summary of future needs, Int. J. Wildland Fire 23 (2014) 295–308.
[11] D. Drysdale, An introduction to fire dynamics, 3rd ed., Wiley, Chichester, West Sussex, 2011.
[12] A.L. Sullivan, Wildland surface fire spread modelling, 1990–2007. 1: physical and quasi-physical models, Int. J. Wildland Fire 18 (2009) 349–368.
[13] J. Lozano, W. Tachajapong, H. Pan, A. Swanson, C. Kelley, M. Princevac, S. Mahalingam, Experimental investigation of the velocity field in a controlled wind-aided propagating fire using particle image velocimetry, Fire Saf. Sci. 9 (2008) 255–266.
[14] J. Lozano, W. Tachajapong, D.R. Weise, S. Mahalingam, M. Princevac, Fluid dynamic structures in a fire environment observed in laboratory-scale experiments, Combust. Sci. Technol. 182 (2010) 858–878.
[15] M.A. Finney, J.D. Cohen, J.M. Forthofer, S.S. McAllister, M.J. Gollner, D.J. Gorham, K. Saito, N.K. Akafuah, B.A. Adam, J.D. English, Role of buoyant flame dynamics in wildfire spread, Proc. Natl. Acad. Sci. (2015) 201504498.
[16] R.M. Nelson Jr., In Memory - George M. Byram - 1909–1996, Int. J. Wildland Fire 6 (1996) 216.
[17] G.M. Byram, Combustion of forest fuels, in: K.P. Davis (Ed.), Forest Fire Control Use, 1st ed., McGraw-Hill, New York, 1959, pp. 61–89.
[18] M.E. Alexander, Calculating and interpreting forest fire intensities, Can. J. Bot. 60 (1982) 349–357.
[19] M.E. Alexander, M.G. Cruz, Interdependencies between flame length and fireline intensity in predicting crown fire initiation and crown scorch height, Int. J. Wildland Fire 21 (2012) 95.
[20] D.R. Weise, E. Koo, X. Zhou, S. Mahalingam, F. Morandini, J.-H. Balbi, Fire spread in chaparral - a comparison of laboratory data and model predictions in burning live fuels, Int. J. Wildland Fire 25 (2016) 980–994.
[21] J.A. Vega, P. Cuiñas, T. Fontúrbel, P. Pérez-Gorostiaga, C. Fernández, Predicting fire behaviour in Galician (NW Spain) shrubland fuel complexes, Proc. 3rd Int. Conf. Forest Fire Res. 14th Conf. Fire For. Meteorol, Coimbra, Portugal, University of Coimbra (1998), pp. 713–728.
[22] G.M. Byram, Forest fire behavior, in: K.P. Davis (Ed.), Forest Fire Control Use, 1st ed., McGraw-Hill, New York, NY, 1959, pp. 89–123.
[23] G.M. Byram, Scaling laws for modeling mass fires, Pyrodynamics 4 (1966) 271–284.
[24] R.M. Nelson Jr., Power of the fire—a thermodynamic analysis, Int. J. Wildland Fire 12 (2003) 51–65.
[25] P.H. Thomas, Some aspects of the growth and spread of fire in the open, Forestry 40 (1967) 139–164.
[26] F.A. Albini, A model for the wind-blown flame from a line fire, Combust. Flame 43 (1981) 155–174.
[27] R.M. Nelson Jr., Byram's energy criterion for wildland fires: units and equations, USDA Forest Service, Intermountain Research Station, Ogden, UT, 1993.
[28] T.L. Clark, M.A. Jenkins, J.L. Coen, D.R. Packham, A coupled atmosphere-fire model: role of the convective Froude number and dynamic fingering at the fireline, Int. J. Wildland Fire 6 (1996) 177–190.
[29] D.R. Weise, G.S. Biging, Effects of wind velocity and slope on flame properties, Can. J. For. Res. 26 (1996) 1849–1858.
[30] R.M. Nelson Jr., Flame characteristics for fires in southern fuels, USDA Forest Service, Southeastern Forest Experiment Station, Asheville, NC, 1980.
[31] E.E. Zukoski, T. Kubota, B. Cetegen, Entrainment in fire plumes, Fire Saf. J. 3 (1981) 107–121.
[32] Y. Hasemi, M. Nishihata, Fuel shape effect on the deterministic properties of turbulent diffusion flames, Fire Saf. Sci. 2 (1989) 275–284.
[33] L.-M. Yuan, G. Cox, An experimental study of some line fires, Fire Saf. J. 27 (1996) 123–139.
[34] F. Morandini, X. Silvani, L. Rossi, P.-A. Santoni, A. Simeoni, J.-H. Balbi, J.L. Rossi, T. Marcelli, Fire spread experiment across Mediterranean shrub: influence of wind on flame front properties, Fire Saf. J. 41 (2006) 229–235.
[35] D. Morvan, A numerical study of flame geometry and potential for crown fire initiation for a wildfire propagating through shrub fuel, Int. J. Wildland Fire 16 (2007) 511–518.
[36] D. Morvan, Physical phenomena and length scales governing the behaviour of wildfires: a case for physical modelling, Fire Technol. 47 (2011) 437–460.
[37] F. Morandini, X. Silvani, Experimental investigation of the physical mechanisms governing the spread of wildfires, Int. J. Wildland Fire 19 (2010) 570–582.
[38] J.E. Keeley, Chaparral, in: M.G. Barbour, W.D. Billings (Eds.), North American Terrestrial Vegetation, 2nd ed., Cambridge University Press, New York, NY, 2000, pp. 203–253.
[39] W.J. Cole, M.H. Dennis, T.H. Fletcher, D.R. Weise, The effects of wind on the flame characteristics of individual leaves, Int. J. Wildland Fire 20 (2011) 657–667.
[40] L. Sun, X. Zhou, S. Mahalingam, D.R. Weise, Comparison of burning characteristics of live and dead chaparral fuels, Combust. Flame 144 (2006) 349–359.
[41] X. Zhou, D. Weise, S. Mahalingam, Experimental measurements and numerical modeling of marginal burning in live chaparral fuel beds, Proc. Combust. Inst. 30 (2005) 2287–2294.
[42] X. Zhou, S. Mahalingam, D. Weise, Experimental study and large eddy simulation of effect of terrain slope on marginal burning in shrub fuel beds, Proc. Combust. Inst. 31 (2007) 2547–2555.
[43] S.L. Stephens, D.R. Weise, D.L. Fry, R.J. Keiffer, J. Dawson, E. Koo, J. Potts, P.J. Pagni, Measuring the rate of spread of chaparral prescribed fires in northern California, Fire Ecol. 4 (2008) 74–86.
[44] T.H. Fletcher, B.M. Pickett, S.G. Smith, G.S. Spittle, M.M. Woodhouse, E. Haake, D.R. Weise, Effects of moisture on ignition behavior of moist California chaparral and Utah leaves, Combust. Sci. Technol. 179 (2007) 1183–1203.
[45] B.L. Yashwanth, B. Shotorban, S. Mahalingam, C.W. Lautenberger, D.R. Weise, A numerical investigation of the influence of radiation and moisture content on pyrolysis and ignition of a leaf-like fuel element, Combust. Flame 163 (2016) 301–316.
[46] J.D. Engstrom, J.K. Butler, S.G. Smith, L.L. Baxter, T.H. Fletcher, D.R. Weise, Ignition behavior of live California chaparral leaves, Combust. Sci. Technol. 176 (2004) 1577–1591.
[47] B.M. Pickett, C. Isackson, R. Wunder, T.H. Fletcher, B.W. Butler, D.R. Weise, Experimental measurements during combustion of moist individual foliage samples, Int. J. Wildland Fire 19 (2010) 153–162.
[48] B.M. Pickett, S.G. Smith, T.H. Fletcher, D.R. Weise, Burning characteristics of live California chaparral and Utah leaf samples, American Meteorological Society, Canmore, Alberta, Canada (2005), p. 9.
[49] W.L. Fons, H.D. Bruce, W.Y. Pong, A steady-state technique for studying the properties of free-burning wood fires, International Symposium on the Use of Models in Fire Research, Washington, D.C., National Academy of Sciences, National Research Council (1961), pp. 219–234. Publication 786.
[50] S. McAllister, M. Finney, The effect of wind on burning rate of wood cribs, Fire Technol. 52 (2016) 1035–1050.
[51] J. Li, S. Mahalingam, D.R. Weise, Chaparral shrub bulk density and fire behavior, USDA Forest Service Research Data Archive, Fort Collins, CO, 2016.
[52] J. Li, S. Mahalingam, D.R. Weise, Experimental investigation of fire propagation in single live shrubs, Int. J. Wildland Fire 26 (2017) 58–70.
[53] S. Hosseini, M. Shrivastava, L. Qi, D.R. Weise, D.R. Cocker, J.W. Miller, H.S. Jung, Effect of low-density polyethylene on smoke emissions from burning of simulated debris piles, J. Air Waste Manag. Assoc. (2014).
[54] W. Tachajapong, Understanding crown fire initiation via experimental and computational modelling, PhD Thesis, University of California Riverside, 2008.
[55] W. Tachajapong, J. Lozano, S. Mahalingam, D.R. Weise, Experimental modelling of crown fire initiation in open and closed shrubland systems, Int. J. Wildland Fire 23 (2014) 451–462.
[56] A. Dahale, S. Ferguson, B. Shotorban, S. Mahalingam, Effects of distribution of bulk density and moisture content on shrub fires, Int. J. Wildland Fire 22 (2013) 625–641.
[57] S. Padhi, B. Shotorban, S. Mahalingam, Computational investigation of flame characteristics of a non-propagating shrub fire, Fire Saf. J. 81 (2016) 64–73.
[58] D.R. Weise, X. Zhou, S. Mahalingam, J. Chong, Marginal fire spread in live fuel beds - horizontal fuels, USDA Forest Service Research Data Archive, Fort Collins, CO, 2015.
[59] D.R. Weise, E. Koo, X. Zhou, S. Mahalingam, A laboratory-scale comparison of rate of spread model predictions using chaparral fuel beds – preliminary results, in: D.D. Wade, M.L. Robinson (Eds.), Proc. 3rd Fire Behav. Fuels Conf., Birmingham, AL, International Association of Wildland Fire (2011), p. 17.
[60] R.M. Nelson Jr., An effective wind speed for models of fire spread, Int. J. Wildland Fire 11 (2002) 153–161.
[61] B.M. Pickett, Effects of moisture on combustion of live wildland forest fuels, Ph.D. thesis, Brigham Young University, 2008.
[62] R.M. Nelson Jr., Water Relations of Forest Fuels, in: E.A. Johnson, K. Miyanishi (Eds.), Forest Fires Behavior and Ecological Effects, Academic Press, San Diego, CA, 2001, pp. 79–149.
[63] G.M. Byram, R.M. Nelson Jr., An analysis of the drying process in forest fuel material, USDA Forest Service, Southern Research Station, Asheville, NC, 2015.
[64] W.L. Fons, H.B. Clements, P.M. George, Scale effects on propagation rate of laboratory crib fires, Symp. (Int.) Combust. 9 (1963) 860–866.
[65] P.H. Thomas, The size of flames from natural fires, Symp. (Int.) Combust. 9 (1963) 844–859.
[66] F.A. Albini, Thermochemical properties of flame gases from fine wildland fuels, USDA Forest Service, Intermountain Forest and Range Experiment Station, Ogden, UT, 1980.
[67] A.A. Putnam, A model study of wind-blown free-burning fires, Symp. (Int.) Combust. 10 (1965) 1039–1046.
[68] R.M. Nelson Jr., C.W. Adkins, Flame characteristics of wind-driven surface fires, Can. J. For. Res. 16 (1986) 1293–1300.
[69] P.M. Fernandes, H.S. Botelho, F.C. Rego, C. Loureiro, Empirical modelling of surface fire behaviour in maritime pine stands, Int. J. Wildland Fire 18 (2009) 698.
[70] S.C. Ferguson, A. Dahale, B. Shotorban, S. Mahalingam, D.R. Weise, The role of moisture on combustion of pyrolysis gases in wildland fires, Combust. Sci. Technol. 185 (2013) 435–453.
[71] H.E. Anderson, R.C. Rothermel, Influence of moisture and wind upon the characteristics of free-burning fires, Symp. (Int.) Combust. 10 (1965) 1009–1019.
[72] R.C. Rothermel, H.E. Anderson, Fire spread characteristics determined in the laboratory, USDA Forest Service, Intermountain Forest and Range Experiment Station, Ogden, UT, 1966.
[73] R.L. Mason, R.F. Gunst, J.L. Hess, Statistical design and analysis of experiments: with applications to engineering and science, Wiley, New York, 1989.
[74] E.E. Zukoski, Properties of fire plumes, in: G. Cox (Ed.), Combustion Fundamentals of Fire, Academic Press, San Diego, CA, 1995, pp. 101–219.
[75] E. Zukoski, Fluid dynamic aspects of room fires, Fire Saf. Sci. 1 (1986) 1–30.
[76] G. Heskestad, Luminous heights of turbulent diffusion flames, Fire Saf. J. 5 (1983) 103–108.
[77] G. Heskestad, On Q^* and the dynamics of turbulent diffusion flames, Fire Saf. J. 30 (1998) 215–227.

[78] F.A. Heinsch, P.L. Andrews, BehavePlus fire modeling system, version 5.0: design and features, USDA Forest Service, Rocky Mountain Research Station, Fort Collins, CO, 2010.
[79] M.A. Finney, FARSITE: Fire Area Simulator– Model Development and Evaluation, USDA Forest Service, Rocky Mountain Research Station, Fort Collins, CO, 1998.
[80] V. Babrauskas, Effective heat of combustion for flaming combustion of conifers, Can. J. For. Res. 36 (2006) 659–663.
[81] A. Pewsey, M. Neuhäuser, G.D. Ruxton, Circular statistics in R, 1st ed., Oxford University Press, Oxford; New York, 2013.
[82] F. Tasdan, O. Yeniay, A comparative simulation of multiple testing procedures in circular data problems, J. Appl. Stat. (2016) 1–15.
[83] R.M. Nelson, Re-analysis of wind and slope effects on flame characteristics of Mediterranean shrub fires, Int. J. Wildland Fire 24 (2015) 1001–1007.
[84] N.I. Fisher, Statistical analysis of circular data, University Press, Cambridge, 1993 Repr., 1. Paperback ed.
[85] D.C. Carslaw, K. Ropkins, openair–an R package for air quality data analysis, Environ. Model. Softw. 27-28 (2012) 52–61.
[86] L. Magee, R^2 measures based on Wald and likelihood ratio joint significance tests, Am. Stat. 44 (1990) 250.
[87] J.G. Eisenhauer, Regression through the origin, Teach. Stat. 25 (2003) 76–80.
[88] R Core Team, R: a language and environment for statistical computing, R Foundation for Statistical Computing, Vienna, Austria, 2015.
[89] P.E. Dennison, M.A. Moritz, Critical live fuel moisture in chaparral ecosystems: a threshold for fire activity and its relationship to antecedent precipitation, Int. J. Wildland Fire. 18 (2009) 1021–1027.
[90] D.R. Weise, R.A. Hartford, L. Mahaffey, Assessing live fuel moisture for fire management applications, in: T.L. Pruden, L.A. Brennan (Eds.), Tall Timbers Fire Ecol. Conf., Tallahassee, FL, Tall Timbers Research Station (1998), pp. 49–55.
[91] C.M. Countryman, Moisture in living fuels affects fire behavior, Fire Manag. 35 (1974) 10–14.
[92] D.A. Stow, P.J. Riggan, E.J. Storey, L.L. Coulter, Measuring fire spread rates from repeat pass airborne thermal infrared imagery, Remote Sens. Lett. 5 (2014) 803–812.
[93] J.L. Coen, P.J. Riggan, Simulation and thermal imaging of the 2006 Esperanza Wildfire in southern California: application of a coupled weather–wildland fire model, Int. J. Wildland Fire 23 (2014) 755–770.
[94] C.M. Countryman, C.W. Philpot, Physical characteristics of chamise as a wildland fuel, USDA Forest Service, Pacific Southwest Forest and Range Experiment Station, Berkeley, CA, 1970.
[95] V.M.R. Muggeo, Estimating regression models with unknown break-points, Stat. Med. 22 (2003) 3055–3071.
[96] J.-H. Balbi, J.-L. Rossi, T. Marcelli, P.-A. Santoni, A 3D physical real-time model of surface fires across fuel beds, Combust. Sci. Technol. 179 (2007) 2511–2537.
[97] J.H. Balbi, F. Morandini, X. Silvani, J.B. Filippi, F. Rinieri, A physical model for wildland fires, Combust. Flame 156 (2009) 2217–2230.
[98] R.M. Nelson Jr., B.W. Butler, D.R. Weise, Entrainment regimes and flame characteristics of wildland fires, Int. J. Wildland Fire 21 (2012) 127–140.
[99] R.I. Emori, K. Saito, A study of scaling laws in pool and crib fires, Combust. Sci. Technol. 31 (1983) 217–231.